THE ASTROPHYSICAL JOURNAL, 514:272–286, 1999 March 20

LONG-TERM SCINTILLATION STUDIES OF PULSARS. III. TESTING THEORETICAL MODELS OF REFRACTIVE SCINTILLATION

N. D. RAMESH BHAT, A. PRAMESH RAO, AND YASHWANT GUPTA
National Centre for Radio Astrophysics, Tata Institute of Fundamental Research, Post Bag 3, Ganeshkhind, Pune-411 007, India
Received 1998 April 20; accepted 1998 October 26

ABSTRACT

Refractive interstellar scintillation (RISS) is thought to be the cause behind a variety of phenomena seen at radio wavelengths in pulsars and compact radio sources. Though there are substantial observational data to support several observable consequences of it, the quantitative predictions from theories have not been thoroughly tested. In this paper, data from our long-term scintillation study of 18 pulsars in the DM range 3–35 pc cm^{-3} are used to test the relevant theoretical predictions. The variabilities of decorrelation bandwidth (v_d), scintillation timescale (τ_d), and flux density (F) are examined for their cross-correlation properties and compared with the existing predictions. The theory predicts a strong correlation between the fluctuations of v_d and τ_d and strong anticorrelations between those of v_d and F, and τ_d and F. For five pulsars, we see a reasonable agreement with the predictions. There is considerable difficulty in reconciling the results for the rest of the pulsars, most of which show the positive correlation between v_d and τ_d but are characterized by poor flux correlations. In general, the measured correlations are lower than the predicted values. Our analysis shows that while the underlying noise sources can sometimes reduce the degree of correlation, they cannot give rise to an absence of correlation. It is also unlikely that the observed poor flux correlations arise from a hitherto unrecognized form of intrinsic flux variations of pulsars. For PSR B0834+06, which shows anomalous behavior in the form of persistent drift slopes, positive correlation is found between τ_d and the drift-corrected v_d. Many pulsars show an anticorrelation between the fluctuations of v_d and the drift rate of intensity patterns, and this is in accordance with simple minded expectations from theory. The detections of correlations between the fluctuations of different observables and a reasonable agreement seen between the predicted and measured correlations for some pulsars confirm RISS as the primary cause of the observed fluctuations. However, the complexity seen with the detailed results suggests the necessity of more comprehensive theoretical treatments for describing refractive fluctuations and their cross-correlations.

Subject headings: ISM: general — pulsars: general — scattering — turbulence

1. INTRODUCTION

With the recognition of interstellar propagation effects in the long-term pulsar flux variations (Sieber 1982), a new class of scintillation, namely refractive interstellar scintillation (RISS), emerged in radio astronomy (Rickett, Coles, & Bourgois 1984). Since then, much progress has been made, both in theoretical as well as observational fronts, to understand this new form of scintillation. RISS is thought to arise from propagation through large-scale (scale sizes $\gtrsim 10^{11}$ m) electron density inhomogeneities in the interstellar medium (ISM) and hence forms a powerful tool to probe the ISM at such scales (see Rickett 1990 for a review). The growing interest in RISS over the recent years is largely motivated from its applicability beyond the field of pulsars and valuable insights it provides to the distribution of electron density irregularities in the ISM. RISS is also investigated with a view to distinguish between the intrinsic and extrinsic effects on signals from pulsars and compact radio sources and for an improved understanding of strong scattering phenomena at radio wavelengths. Most investigations of RISS effects have been, so far, largely based on observations of pulsars. Owing to their high spatial coherence and pulsed nature of radiation, pulsars are expected to exhibit a variety of observable effects due to RISS.

Various observable effects of interstellar scattering (ISS) on pulsar signals can be classified into (1) diffractive effects, (2) refractive effects, and (3) combined effects due to diffraction and refraction. Detailed theoretical treatments can be found in Cordes, Pidwerbetsky, & Lovelace (1986) and Romani, Narayan, & Blandford (1986) (also see Rickett 1990; Narayan 1992; and Hewish 1992 for reviews). The refractive effects include, in addition to the familiar long-term (days to weeks at meter wavelengths) flux variations, modulations of diffractive interstellar scintillation (DISS) observables, drifting of intensity patterns, timing perturbations, and image wandering. The combined effects of diffraction and refraction in the ISM can, occasionally, give rise to dramatic events, in the form of periodic intensity modulations in time and frequency, which form potential tools to probe pulsar magnetospheres (see, e.g., Wolszczan & Cordes 1987). RISS is also thought to be the cause behind slow (months to years) flux variations (mainly at meter wavelengths) seen with a number of compact extragalactic radio (EGR) sources and unusual flux variations, known as extreme scattering events (ESE), seen with some quasars (at centimeter wavelengths) (see, e.g., Bondi et al. 1994; Spangler et al. 1993; Fiedler et al. 1987, 1994). However, unlike DISS, there are several aspects of RISS phenomena that remain to be well understood (see Rickett 1990; Cordes, Rickett, & Backer 1988a).

Properties of various kinds of observables of interest in the ISS of pulsars are discussed by Cordes et al. (1986) and Romani et al. (1986). The effects investigated by them include modulations of diffraction patterns, fluctuations in pulse arrival times, drifting bands in dynamic spectra, multiple imaging, angular wandering and distortion of scattered images, and the well-known long-term flux variations. In the formalism of Romani et al. (1986), refraction effects

are treated as weak perturbations of a bundle of rays scatter-broadened by small-scale density inhomogeneities. The small- and large-scale inhomogeneities are assumed to be part of a power-law form of spectrum, and the scattering model considered is a thin screen placed between the source and the observer. They extend this formalism to compute the auto- and cross-correlation functions of different observables analytically. The explicit predictions of cross-correlations given by them for the fluctuations of flux and DISS observables (v_d and τ_d) are particularly suitable for experimental verifications. Cordes et al. (1986) consider a phase screen comprising the "slow" and "rapid" components of phase fluctuations and employ a formalism based on the Kirchoff diffraction integral. Refractive effects are analyzed using a Taylor expansion of the "slow" component. They do not make any quantitative predictions of correlation properties, but the formalism can be extended to make the relevant predictions.

Although models based on simple power-law spectra for density fluctuations and a single phase screen appear to be simplistic to describe much more complicated scenarios of ISS, it is worthwhile testing the explicit predictions of such models for the following reasons. First, cross-correlations between the fluctuations of observables form more direct and rigorous tests of the RISS theory. Second, it is necessary to examine critically to what extent the observations support the predictions of simple models, the results from which would provide valuable inputs for suitable refinements of the models.

A number of observational attempts have been made in the recent past toward investigating basic consequences of RISS such as long-term flux variations of pulsars (see, e.g., Kaspi & Stinebring 1992; Gupta, Rickett, & Coles 1993) and the changing form of pulsar dynamic spectra (see, e.g., Gupta, Rickett, & Lyne 1994; Bhat, Rao, & Gupta 1998). But only a few observational studies have been made to verify the predicted cross-correlation properties between the scintillation observables. To the best of our knowledge, there have been only two instances of such attempts. Recent timing observations of the millisecond pulsar PSR B1937+21 yield some evidence supporting the theoretical predictions (Lestrade, Cognard, & Biraud 1995). An anti-correlation between the flux variations and times of arrival is reported, which is found to be consistent with the prediction for a density spectrum with power-law index $\alpha < 4$. Also, observations of PSR B0329+54 by Stinebring, Faison, & McKinnon (1996) showed that the correlation properties between variations of flux, decorrelation bandwidth, and scintillation time are in agreement with the theoretical predictions. Given the complexity of ISS, these examples may not necessarily represent the typical behavior. It is highly desirable to test the predictions for a large number of pulsars so that the possibility of an observational bias can be reduced. Such extensive tests have not been carried out so far.

We have carried out a long-term systematic study of the scintillation properties of 18 pulsars using the Ooty Radio Telescope (ORT) at 327 MHz during a 3 yr period from 1993 to 1995. One of the prime objectives was to study refractive effects in pulsar scintillation. The dynamic scintillation spectra of pulsars were regularly monitored for 10–90 epochs over time spans $\sim$100–900 days, from which scintillation parameters, viz., decorrelation bandwidth (v_d), scintillation timescale (τ_d), frequency drift rate (dt/dv), and pulsar flux density (F), were measured. Details of observations and results on diffractive and refractive scintillation properties have been discussed in an earlier paper (Bhat et al. 1999a, hereafter Paper I). The results were also used to study the distribution of scattering material in the local interstellar medium (LISM) (Bhat, Gupta, & Rao 1998) and to investigate the form of the electron density spectrum in the ISM (Bhat, Gupta, & Rao 1999b, hereafter Paper II). The results from a cross-correlation analysis of the fluctuations of various parameters are presented in this paper. We give a brief review of the relevant theory in § 2. Our data analysis and results are presented in § 3. In § 4, we compare the results with the theoretical predictions. In § 5, we discuss some of the possibilities of reconciling the observations and theories. Our conclusions are summarized in § 6.

2. THEORETICAL BACKGROUND

Although several papers have addressed different issues related to refractive scintillation effects, we find that two papers, Cordes et al. (1986) and Romani et al. (1986), contain theoretical treatments relevant to our investigations. Despite the differences in the details, both papers attempt to explain a variety of effects on scintillation observables that can be caused by RISS. The authors rely on ray-tracing techniques to explain refractive effects and wave techniques for diffractive effects. The scattering model considered is that of a thin screen placed between the source and the observer.

Cordes et al. (1986) analyzed refractive effects using a Taylor expansion of the "slow" component of phase perturbations, sometimes termed the "refractive phase" $\phi_{\rm ref}$, which varies over length scales $\sim$ "multipath scale" ($r_{\rm mp} \sim Z\theta_{\rm diff}$, where Z is the distance to the scattering screen and $\theta_{\rm diff}$ is the diffractive scattering angle). The refraction-induced fluctuations of scintillation parameters are treated in terms of "gradient" and "curvature" components of this refractive phase. The observables such as spatial scale (s_d) and characteristic bandwidth (v_d) of scintillation patterns, the mean flux density (F), and the drift rate (dt/dv) of patterns are expressed in terms of refraction angle, $\theta_{\rm ref}$, and a "gain" term, G, which are defined as

$$\theta_{\rm ref} = \frac{\lambda}{2\pi}\left(\frac{\partial\phi_{\rm ref}}{\partial r}\right) \quad \text{and} \quad G = \left(1 + \frac{\lambda Z}{2\pi}\frac{\partial^2\phi_{\rm ref}}{\partial r^2}\right)^{-1}. \tag{1}$$

According to the relations given by Cordes et al. (1986), the refractive modulations of spatial scale (or, alternatively, the scintillation timescale, τ_d) and flux density (F) are governed by the gain term (G), whereas the decorrelation bandwidth (v_d) is modulated by both $\theta_{\rm ref}$ as well as G. Modulations of the drift slope are due to variations of $\theta_{\rm ref}$. Therefore, it is reasonable to expect variabilities of diffractive scintillation parameters and the flux density to be interrelated to each other. For example, larger values of G increase the apparent flux, whereas the scintillation time is reduced by a similar factor. The variability of v_d is expected to be rather complicated, as demonstrated by their numerical simulations. However, the authors do not make any quantitative, verifiable predictions of correlation properties of these parameters.

Romani et al. (1986) treat refraction-induced fluctuations as weak perturbations of a bundle of rays scatter-broadened by the short-wavelength electron density inhomogeneities.

The source image is assumed to arise from a Gaussian-shaped bundle of such rays, which get focused, defocused, or steered by the density profiles over length scales $\sim Z\theta_{\rm diff}$ (which is also the "image size" on the phase screen). As in the work of Cordes et al. (1986), large-scale phase variations give rise to a refractive bending angle, $\theta_{\rm ref}$. The assumption of weak perturbations essentially means the refractive displacements of the ray bundle, given by $X \sim Z\theta_{\rm ref}$, are small compared to the image size, $Z\theta_{\rm diff}$, which, in turn, implies a refractive bending angle that is smaller than the small-scale scattering angle ($\theta_{\rm ref} < \theta_{\rm diff}$). Based on this formalism, fractional fluctuations of observables of interest, such as the source size Ω, v_d, τ_d, F, etc., are calculated by integrating "intensity-weighted" $\phi_{\rm ref}$ over the image size (see Blandford & Narayan 1985 for a detailed discussion). The weighting function depends on the observable. The mean auto- and cross-correlations are computed for the observables using the Fourier transform method (see Appendix A of Romani et al. 1986 for details). The authors group the variabilities of scintillation parameters into two classes, viz., (1) curvature-induced and (2) gradient-induced, and argue that, in general, one can expect the quantities belonging to a particular class to covary among themselves and the quantities of different classes to show dissimilar variations. They emphasize that fluctuations of three quantities, viz., decorrelation bandwidth, scintillation time, and flux, are most suitable for observational verification and suggest that detections of such fluctuations, particularly their cross-correlations, will help toward understanding the refractive scintillation effects in the ISM.

In this paper, we restrict ourselves to the observables that can be obtained from our data. Of five quantities that can be measured from the dynamic spectrum at a given epoch—v_d, τ_d, dt/dv, F, and the scintillation index (m_d), there are clear predictions made by Romani et al. (1986) for the cross-correlation properties of v_d, τ_d, and F. It should be mentioned that the scattering model considered by them employs a single-phase screen and a simple power-law description for the underlying density fluctuations. This may be an idealized simplification of the real situation. We have summarized these predictions in Table 1 in terms of zero-lag correlation coefficients for three different types of density spectra with power-law indices (α) of 11/3, 4, and 4.3. In general, the observable effects of refractive scintillation are thought to be strongly dependent on the form of the density spectrum, but the predicted correlation properties between the fluctuations of v_d, τ_d, and F change only marginally with α. To summarize their predictions, a high positive correlation (0.75–0.79) is expected between variations of decorrelation bandwidth and scintillation time, whereas high anticorrelations are expected between variations of decorrelation bandwidth and flux (-0.76 to -0.84) and those of scintillation time and flux (-0.50 to -0.64).

3. DATA ANALYSIS AND RESULTS

The theoretical predictions described above can be tested using the pulsar scintillation data presented in Paper I. Time series of four parameters—decorrelation bandwidth (v_d), scintillation timescale (τ_d), drift rate of intensity patterns (dt/dv), and flux density (F)—for each pulsar are presented in Figures 4*a*–4*x* of Paper I. Our observations show large-amplitude fluctuations of these quantities; typically 40%–50% fluctuations for v_d and F, 20%–30% for τ_d, and rms fluctuations of a few s kHz^{-1} for dt/dv (Paper II). The dynamic spectra are found to vary significantly over timescales as short as 2–3 days, which, to first order, is in accord with basic expectations of refractive modulations at our observing frequency (Paper I). However, while the modulations of scintillation observables v_d, τ_d, dt/dv, and pulsar flux density (F) due to refractive scintillation effects in the ISM have been detected, the depths of modulations are found to be much larger than the expectations of a Kolmogorov-type density spectrum (see Paper II). In this paper, we present a correlation analysis of this data set and examine how well the results are in agreement with the existing theoretical predictions.

In addition to studying the correlation properties between the fluctuations of v_d, τ_d, and F, for which theoretical predictions exist, we also examine the correlation properties between the fluctuations of v_d and dt/dv. The motivation for this is as follows. According to the current models of refractive scintillation, the "apparent" or "instantaneous" decorrelation bandwidth (v_d) is expected to be less than the characteristic bandwidth (v_{d_o}) (i.e., v_d in the absence of refraction effects) when the refractive bending angle is significant (see Cordes et al. 1986; Gupta et al. 1994). Our observations (Paper II) show that there are considerable variations of $\theta_{\rm ref}$ (rms refractive angle $\delta\theta_{\rm ref} \sim 1$ mas) over the observing time spans (typically $\sim$100 days). Therefore, it is reasonable to expect variations of $\theta_{\rm ref}$ (or, alternatively, the gradient component of the slowly varying phase $\phi_{\rm ref}$) to play a substantial role in the long-term modulation characteristics of v_d. To examine the possible connection between the two effects, we carry out a correlation analysis between v_d and dt/dv. Since the modulations of v_d are insensitive to the sign of the drift slope (see Gupta et al. 1994 and Cordes et al. 1986 for details), we correlate variations of v_d with those of $|dt/dv|$.

The pulsars and the periods of observation are tabulated in columns (2) and (3) of Table 2. Columns (4) and (5) of Table 2 give the number of epochs of observation ($N_{\rm ep}$) and the time span of data ($T_{\rm sp}$), respectively. For pulsars PSR B0823+26, PSR B0834+06, PSR B1133+16, and PSR B1919+21, there are multiple entries, which correspond to data from different observing sessions. The symbols I–IV, when attached alongside pulsar names, indicate the data

TABLE 1

PREDICTED CORRELATION COEFFICIENTS FROM ROMANI ET AL. (1986)

Power-Law Index α (1)	Decorrelation Bandwidth and Scintillation Timescale $\{v_d, \tau_d\}$ (2)	Decorrelation Bandwidth and Flux Density $\{v_d, F\}$ (3)	Scintillation Timescale and Flux Density $\{\tau_d, F\}$ (4)
11/3	0.75	−0.76	−0.50
4	0.77	−0.80	−0.58
4.3	0.79	−0.84	−0.64

TABLE 2

PULSAR SAMPLE: OBSERVING PARAMETERS AND CLASSIFICATION

Number (1)	Pulsar (Session) (2)	Period of Observation (3)	N_{ep} (4)	T_{sp} (days) (5)	Drift Class[a] (6)	LOS Class[b] (7)
1.....	PSR B0329+54	1995 Apr–Jul	14	66	NC	A
2.....	PSR B0628−28	1993 Oct–1994 Jan	17	83	I	B
3.....	PSR B0823+26(I)	1993 Mar–May	12	66	I	C
4.....	PSR B0823+26(II)	1993 Oct–1994 Jan	19	87	NC	...
5.....	PSR B0834+06(I)	1993 Jan–May	27	120	II	C
6.....	PSR B0834+06(II)	1993 Oct–1994 Jan	18	74	II	...
7.....	PSR B0834+06(III)	1994 Feb–Jun	21	78	II	...
8.....	PSR B0834+06(IV)	1995 Apr–Jul	27	100	I	...
9.....	PSR B0919+06	1994 Mar–Jun	19	70	I	C
10	PSR B1133+16(I)	1993 Jan–Feb	6	19	I	D
11	PSR B1133+16(II)	1994 Feb–Jun	25	90	I	...
12	PSR B1133+16(III)	1995 Apr–Jul	27	95	NC	...
13	PSR B1237+25	1993 Oct–1994 Jan	9	77	NC	D
14	PSR B1508+55	1995 Apr–Jul	9	52	I	B
15	PSR B1540−06	1995 Apr–Jul	12	91	I	B
16	PSR B1604−00	1995 Apr–Jul	10	93	I	B
17	PSR B1747−46	1995 Apr–Jul	12	92	I	A
18	PSR B1919+21(I)	1993 Mar–May	15	59	II	B
19	PSR B1919+21(II)	1993 Oct–1994 Jan	48	87	II	...
20	PSR B1929+10	1994 Mar–Jun	09	42	I	C
21	PSR B2016+28	1993 Oct –1994 Jan	20	83	I	A
22	PSR B2020+28	1994 Mar–Jun	15	74	I	A
23	PSR B2045−16	1993 Oct –1994 Jan	35	85	NC	B
24	PSR B2310+42	1995 Apr–Jul	10	77	NC	A
25	PSR B2327−20	1994 Mar–Jun	18	68	I	C

[a] Based on the statistical characteristics of drift rate measurements (see Paper II for details).

[b] Based on the scattering geometry of the line of sight (LOS) expected from the model for the local interstellar medium (Bhat et al. 1998).

from a given session (see Tables 1 and 2 of Paper I for details). Though data from each session for these pulsars span a large number of refractive timescales (as per our expected estimates), the results show that the diffractive and refractive scintillation properties sometimes vary significantly between successive sessions (see Papers I and II). Hence, we treat them as independent data sets for the correlation analysis.

Details concerning the statistical quality of our data and possible non-ISS effects that give rise to the modulations of the measured parameters are described in Appendices A and B of Paper II. The correlation properties are meaningful only when the data span several refractive timescales. Rough estimates of the number of refractive cycles of fluctuations (N_{ref}) are given in Table 3 of Paper II. We find that for pulsars PSR B2016+28, PSR B1540−06, and PSR B2310+42, the data span only a few timescales of fluctuations ($N_{ref} \sim 3$), and hence their correlation properties may not be reliable. Also, along the directions of PSR B1540−06 and PSR B1604−00, variation in the transverse component of Earth's orbital motion ($V_{obs\perp}$) contributes substantially to the modulations of the scintillation timescale (τ_d). The expected fractional variation in τ_d due to this (δt_{vobs}) is comparable to the measured modulation index of τ_d (i.e., $\delta t_{vobs} \approx m_t$). Therefore, the τ_d correlations (i.e., between v_d and τ_d, and τ_d and F) of these pulsars may not be meaningful. Owing to their comparatively large fractional linear polarizations ($m_{lin} \sim 0.6$–0.8 at 400 MHz), the flux density modulations (as measured by ORT) of PSR B1237+25 and PSR B1929+10 can get significantly modified by the variable Faraday rotation (due to Earth's ionosphere). Therefore, the flux correlations of these pulsars (i.e., between v_d and F, and τ_d and F) may not be reliable. Although we carry out the correlation analysis for all the 18 pulsars, the results for above-mentioned pulsars should be treated with caution. For the rest of the pulsars, these three effects are not significant.

3.1. *Cross-Correlation Analysis and Results*

Sample data from our observations are shown in Figures 1*a*–1*l* and 2*a*–2*c* in the form of scatter plots of various combinations: v_d versus τ_d, v_d versus F, τ_d versus F, and v_d versus dt/dv. The trends visible therein give some idea of the nature of correlations between different combinations. A full cross-correlation function analysis is not practical with our data owing to the limited number of measurements in the time series of the parameters. Therefore, we compute cross-correlation coefficients, i.e., normalized zero-lag values of cross-correlation functions, for which predictions are readily available. The quantity we use as a measure of the correlation between the parameters is the *Spearman rank-order correlation coefficient* (r_s), which is defined as (see, e.g., Press et al. 1992)

$$r_s = \frac{\sum_i (R_i - \overline{R})(S_i - \overline{S})}{\sqrt{\sum_i (R_i - \overline{R})^2}\sqrt{\sum_i (S_i - \overline{S})^2}}, \quad (2)$$

where R_i and S_i represent the ranks of the two quantities x_i and y_i for which the correlation coefficient is computed and the summation is carried out over the total number of available data points in the time series. The quantities $\overline{R}$ and $\overline{S}$

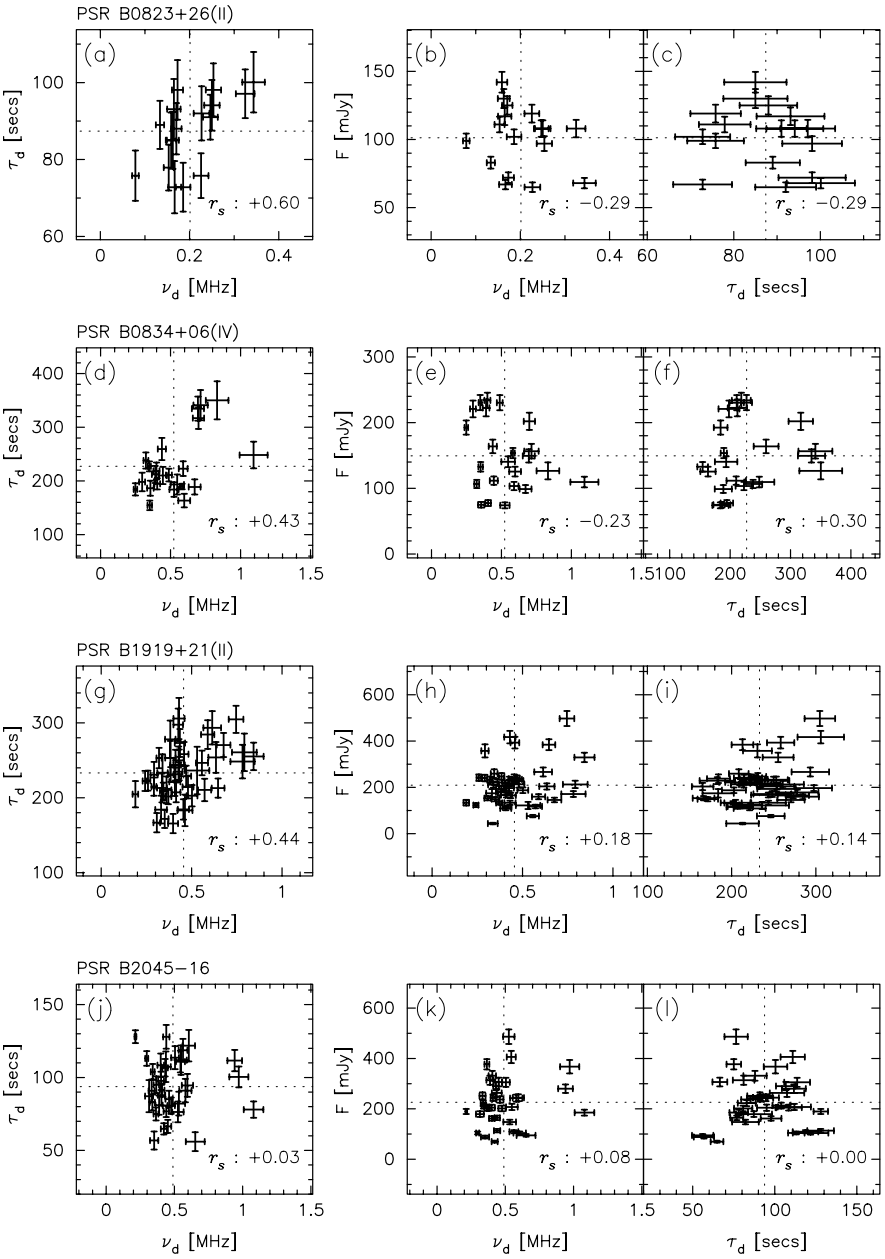

FIG. 1.—Sample scatter plots for different combinations of the quantities ν_d, τ_d, and F, illustrating the diversity seen in the correlation properties and their agreement with the predictions. The pulsar name (with session ID) is given at the top of each panel, and the rank correlation coefficient (r_s) is indicated at the lower right-hand corner. The dotted lines indicate the mean values of the quantities. The data of PSR B0823+26(II) is an example in which all the three correlations are in reasonable agreement. The agreement is only partial for PSR B0834+06(IV) and PSR B1919+21(II); two combinations are in agreement for the former, whereas only a single combination agrees with the prediction for the latter. For PSR B2045−16, all the three quantities are uncorrelated to each other.

denote the average values of R_i and S_i, respectively, over the entire time span of observation. The rank correlation method is preferred over the normally used linear correlation for the following reasons. It is a nonparametric test, in which no assumptions are made about the distributions of the quantities. A nonparametric correlation is more robust than the linear correlation method. In addition, the rank correlation method is less sensitive to outliers than the linear correlation, in which they are likely to introduce a bias in the mean, thereby giving rise to unreliable correlations. The rank correlation test is also applicable in the case of nonlinear dependence between the quantities, unlike the case for linear correlation.

We also computed the linear correlation coefficients (also referred to as "Pearson's r"; Press et al. 1992), which sometimes differ substantially from their rank correlation counterparts and in general have poorer confidence intervals. The results from the two methods, however, are found to be in qualitative agreement. Other methods of examining the relation between two quantities, such as *Kendall*'s *tau* (Press et al. 1992), also give qualitatively similar results. Therefore, we restrict ourselves to the results obtained from the rank correlation technique in the subsequent discussion.

The confidence intervals of the rank correlation coefficients are derived using the "bootstrap" method (Efron 1979; Diaconis & Efron 1983). The procedure is as follows.

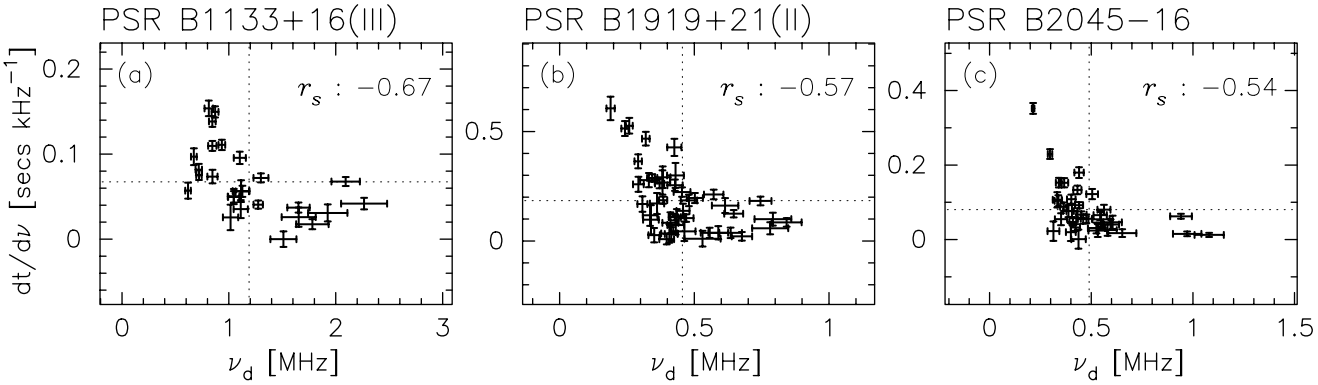

FIG. 2.—Sample scatter plots illustrating the anticorrelation property between the variabilities of v_d and dt/dv. The panel description is similar to that for Fig. 1.

From the observed sample of N_{ep} data points in a given data, a new sample of N_{ep} values is generated by a random rearrangement process. The rank correlation coefficient is computed for this bootstrap sample. This process is repeated a very large number of times, and a probability distribution is created from the coefficients obtained for all the samples. We have made use of 10^5 bootstrap samples generated from the basic data set. Computations for much larger number of samples produce very little changes in the statistical properties of the distribution. The desired confidence intervals are obtained by appropriately integrating over this distribution curve. For instance, if P_{r_s} is the desired confidence level in percentage, then the distribution is integrated from either of the wings inward to $(100 - P_{r_s})/2$ percent of the total area under the distribution curve to get the corresponding limits of the confidence interval. The analysis is carried out for a wide range of intervals (P_{r_s} ranging from 60% to 95%). Owing to the limited number of measurements (N_{ep}) and finite number of independent refractive cycles (N_{ref}) spanned by our data, we prefer 90% levels to decide the significance of our correlation results. The estimated width of the confidence interval reflects, to first order, the statistical quality of our data in terms of N_{ep} and N_{ref} and the uncertainties in individual measurements.

TABLE 3

RESULTS FROM THE CORRELATION ANALYSIS

Number (1)	Pulsar (Session) (2)	$r_s\{v_d, \tau_d\}$ (3)	$r_s\{v_d, F\}$ (4)	$r_s\{\tau_d, F\}$ (5)	$r_s\{v_d, dt/dv\}$ (6)	Remarks[a] (7)
1	PSR B0329+54	$0.04^{+0.45}_{-0.59}$	$0.45^{+0.72}_{-0.31}$	$-0.61^{-0.26}_{-0.94}$	$-0.01^{+0.50}_{-0.70}$	1A
2	PSR B0628−28	$0.52^{+0.75}_{-0.04}$	$-0.36^{+0.00}_{-0.82}$	$-0.70^{-0.44}_{-0.95}$	$-0.41^{+0.05}_{-0.90}$	RA
3	PSR B0823+26(I)	$0.47^{+0.79}_{-0.25}$	$0.09^{+0.41}_{-0.59}$	$-0.03^{+0.29}_{-0.62}$	$-0.38^{+0.05}_{-0.90}$	1A
4	PSR B0823+26(II)	$0.60^{+0.76}_{-0.04}$	$-0.29^{+0.09}_{-0.71}$	$-0.29^{+0.05}_{-0.79}$	$-0.55^{-0.26}_{-0.89}$	RA
5	PSR B0834+06(I)	$0.44^{+0.66}_{+0.09}$	$0.28^{+0.50}_{+0.00}$	$0.37^{+0.59}_{+0.07}$	$-0.18^{+0.12}_{-0.50}$	1A
6	PSR B0834+06(II)	$-0.14^{+0.22}_{-0.58}$	$-0.24^{+0.12}_{-0.62}$	$-0.04^{+0.29}_{-0.42}$	$-0.69^{-0.48}_{-0.90}$	1A
7	PSR B0834+06(III)	$0.07^{+0.44}_{-0.44}$	$-0.07^{+0.23}_{-0.44}$	$-0.02^{+0.32}_{-0.44}$	$-0.30^{+0.09}_{-0.68}$	0A
8	PSR B0834+06(IV)	$0.42^{+0.65}_{+0.01}$	$-0.23^{+0.05}_{-0.53}$	$0.30^{+0.50}_{+0.00}$	$-0.39^{-0.06}_{-0.71}$	2A
9	PSR B0919+06	$0.60^{+0.75}_{+0.25}$	$-0.21^{+0.17}_{-0.68}$	$-0.19^{+0.17}_{-0.65}$	$-0.20^{+0.17}_{-0.59}$	RA
10	PSR B1133+16(I)	$0.42^{+0.88}_{+0.19}$	$-0.37^{+0.17}_{-1.00}$	$-0.09^{+0.34}_{-0.97}$	$-0.43^{+0.22}_{-1.00}$	2A
11	PSR B1133+16(II)	$0.83^{+0.91}_{+0.62}$	$-0.04^{+0.25}_{-0.41}$	$0.01^{+0.32}_{-0.34}$	$-0.37^{-0.08}_{-0.68}$	1A
12	PSR B1133+16(III)	$0.32^{+0.57}_{-0.07}$	$-0.01^{+0.29}_{-0.38}$	$0.09^{+0.35}_{-0.25}$	$-0.67^{-0.50}_{-0.81}$	1A
13	PSR B1237+25[b]	$0.43^{+0.66}_{-0.35}$	$0.86^{+0.97}_{+0.32}$	$0.07^{+0.44}_{-0.70}$	$-0.50^{-0.04}_{-0.96}$	1A
14	PSR B1508+55	$0.40^{+0.62}_{-0.48}$	$-0.57^{-0.02}_{-0.97}$	$-0.86^{-0.75}_{-1.00}$	$-0.38^{+0.28}_{-0.97}$	RA
15	PSR B1540−06[b]	$0.05^{+0.47}_{-0.62}$	$0.43^{+0.65}_{-0.20}$	$-0.07^{+0.41}_{-0.79}$	$-0.56^{-0.23}_{-0.94}$	SC
16	PSR B1604−00[b]	$0.22^{+0.53}_{-0.52}$	$-0.02^{+0.34}_{-0.63}$	$-0.31^{+0.16}_{-0.88}$	$-0.71^{-0.41}_{-0.98}$	2A
17	PSR B1747−46	$0.39^{+0.68}_{-0.22}$	$0.31^{+0.75}_{-0.55}$	$0.32^{+0.55}_{-0.45}$	$0.15^{+0.41}_{-0.41}$	1A
18	PSR B1919+21(I)	$0.21^{+0.47}_{-0.28}$	$0.01^{+0.35}_{-0.48}$	$-0.05^{+0.34}_{-0.56}$	$-0.32^{+0.08}_{-0.75}$	1A
19	PSR B1919+21(II)	$0.39^{+0.58}_{+0.15}$	$0.18^{+0.41}_{-0.08}$	$0.14^{+0.35}_{-0.10}$	$-0.57^{-0.36}_{-0.71}$	1A
20	PSR B1929+10[b]	$0.10^{+0.41}_{-0.81}$	$0.55^{+0.78}_{-0.48}$	$0.19^{+0.42}_{-0.66}$	$-0.33^{+0.12}_{-0.96}$	SC
21	PSR B2016+28[b]	$0.53^{+0.71}_{+0.17}$	$-0.13^{+0.31}_{-0.58}$	$0.30^{+0.69}_{-0.22}$	$-0.69^{-0.44}_{-0.90}$	2A
22	PSR B2020+28	$0.45^{+0.64}_{+0.01}$	$-0.56^{-0.02}_{-0.85}$	$-0.66^{-0.17}_{-0.89}$	$-0.03^{+0.47}_{-0.58}$	RA
23	PSR B2045−16	$0.03^{+0.29}_{-0.25}$	$0.08^{+0.32}_{-0.22}$	$0.00^{+0.31}_{-0.35}$	$-0.54^{-0.31}_{-0.75}$	0A
24	PSR B2310+42[b]	$0.04^{+0.56}_{-0.68}$	$-0.67^{-0.28}_{-0.98}$	$-0.15^{+0.32}_{-0.88}$	$0.13^{+0.77}_{-0.76}$	1A
25	PSR B2327−20	$-0.04^{+0.38}_{-0.68}$	$0.27^{+0.61}_{-0.35}$	$0.40^{+0.70}_{+0.00}$	$0.06^{+0.52}_{-0.56}$	SC

[a] On the agreement with the predictions given in Table 1. RA: reasonable agreement; 2A, 1A, and 0A: 2, 1, and 0 combination(s) is (are) in agreement; SC: spurious correlations.

[b] Correlations may not be reliable, as described in § 3.

It is possible that this method still underestimates the uncertainty when the data do not span many independent cycles of fluctuations and/or the amplitudes do not span the total range of values.

The analysis described above is carried out for the following combinations of the observables: (1) decorrelation bandwidth and scintillation timescale (v_d vs. τ_d), (2) decorrelation bandwidth and flux density (v_d vs. F), (3) scintillation timescale and flux density (τ_d vs. F), and (4) decorrelation bandwidth and drift rate (v_d vs. dt/dv). The results are tabulated in columns (3), (4), (5), and (6), respectively, of Table 3. Pulsars for which our correlation results may not be reliable, due to reasons described earlier, are marked with a footnote. The confidence intervals of the correlation coefficients obtained from the bootstrap method are shown as the subscript (90% lower limit) and the superscript (90% upper limit). Throughout this paper, we use $\{A, B\}$ to refer to the cross-correlation between the quantities A and B, and $r_s\{A, B\}$ to denote its rank correlation coefficient.

Our analysis shows that the correlation properties change significantly from pulsar to pulsar, and the coefficients vary over a very wide range. Excluding the unreliable correlations (see Table 3), $r_s\{v_d, \tau_d\}$ ranges from -0.14 [PSR B0834+06(II)] to 0.83 [PSR B1133+16(II)], $r_s\{v_d, F\}$ from -0.57 (PSR B1508+55) to 0.45 (PSR B0329+54), and $r_s\{\tau_d, F\}$ from -0.86 (PSR B1508+55) to 0.37 [PSR B0834+06(I)]. The values of $r_s\{v_d, dt/dv\}$ range from -0.71 (PSR B1604−00) to 0.15 (PSR B1747−46). There are a large number of data (roughly one-third) for which the magnitudes of correlation coefficients are very low ($|r_s| \lesssim 0.1$), and these will be treated as "insignificant correlations" in our subsequent discussion. The significances of the rest of the correlations are decided purely on the basis of the limits of the confidence intervals. In the discussion that follows, we usually refer to correlation coefficients unless a special mention is made of the confidence limits. In column (7) of Table 3, we indicate the nature of agreement between the correlations and the theoretical predictions.

4. COMPARISON WITH THEORETICAL PREDICTIONS

4.1. *Correlations between DISS Observables and Flux Density*

On comparing Tables 1 and 3, we recognize that there is no pulsar for which results are in complete agreement with the theoretical predictions. Five pulsars show correlation properties in qualitative agreement with the predictions; these are PSR B0628−28, PSR B0823+26(II), PSR B0919+06, PSR B1508+55, and PSR B2020+28. However, the observed correlations are in general lower compared to their predicted values. For PSR B0628−28, the results agree with the predictions within the 90% confidence intervals, whereas a similar agreement is not seen with the other four for all three combinations.

Correlation properties of the remaining data are rather complex. Four data sets show two of the combinations in qualitative agreement, but an absence or an opposite correlation for the third combination (these are indicated by "2A" in col. [7] of Table 3). For 11 data sets (indicated by "1A" in col. [7] of Table 3), only one of the three combinations agrees with the prediction, while an absence [e.g., PSR B1133+16(II) and PSR B0823+26(I)] or an opposite correlation [e.g., PSR B0834+06(I) and PSR B1919+21(II)] is seen for the remaining two combinations. There are also examples [PSR B0834+06(III) and PSR B2045−16] in which the fluctuations of all the three quantities are uncorrelated to each other. Thus, the results vary over a very wide range from a complete absence of correlations to a reasonable agreement within the confidence intervals; in between there are several cases in which the agreement is only partial.

For PSR B1540−06, PSR B1929+10, and PSR B2327−20, the observed correlations are in the opposite sense to that predicted by theory. However, a close inspection of the relevant data reveals that these are spurious correlations arising owing to the nonrandomness of the data (Figs. 4*n*, 4*s*, and 4*x* of Paper I). PSR B1540−06 shows a significant fading between the first and second halves of the data; while the measurements of the first half are consistently biased above the mean value, those of the second half are biased below the mean. Therefore, the observed positive correlation for $\{v_d, F\}$ for this pulsar is not meaningful. As mentioned in § 3, the flux density modulations due to variable Faraday rotation is expected to be substantial for PSR B1929+10 owing to its very large fractional linear polarization ($m_{\rm lin} \sim 0.8$ at 400 MHz; Gould 1994), which makes the observed flux correlations ($r_s\{v_d, F\}$ and $r_s\{\tau_d, F\}$) unreliable. There are some signatures of systematic trends in the time series of v_d and F of PSR B2327−20, which are the probable cause behind the spurious flux correlations seen for this pulsar. The correlations of these three pulsars, therefore, should not be taken seriously.

The diversity seen in the correlation properties is exemplified by Figures 1*a*–1*l*. PSR B0823+26(II) is an example of "reasonable agreement," with $r_s\{v_d, \tau_d\} \approx 0.6$, $r_s\{v_d, F\} \approx -0.3$, and $r_s\{\tau_d, F\} \approx -0.3$, and the corresponding trends are visible in Figures 1*a*–1*c*. For PSR B0834+06(IV) (Figs. 1*d*–1*f*), only two combinations—$r_s\{v_d, \tau_d\} = 0.43$ and $r_s\{v_d, F\} = -0.23$—are in qualitative agreement with the predictions. PSR B1919+21(II) (Figs. 1*g*–1*i*) is an example in which only one combination—$r_s\{v_d, \tau_d\} = 0.44$—agrees with the prediction. The extreme case of variabilities of all three quantities uncorrelated to each other is shown in Figures 1*j*–1*l* through the example of PSR B2045−16.

4.2. *The Anticorrelation between Decorrelation Bandwidth and Drift Slope*

A fairly large number of pulsars in our sample (20 of the 25 entries in Table 3) show an anticorrelation between the fluctuations of v_d and dt/dv. Such a relation can be expected from the effect of refractive bending angle on the intensity decorrelation in frequency (see Cordes et al. 1986; Gupta et al. 1994). Figures 2*a*–2*c* show sample plots illustrating the anticorrelation between v_d and dt/dv. Like other combinations, correlations between v_d and dt/dv also vary over a wide range: from values as low as ≈ -0.2 [e.g., PSR B0919+06 and PSR B0834+06(I)] to ≈ -0.7 [e.g., PSR B0834+06(II) and PSR B1133+16(III)]. If such correlations result from the "phase-gradient–induced" modulations of v_d, then the other bandwidth correlations such as $\{v_d, \tau_d\}$ and $\{v_d, F\}$, which are expected to arise purely from curvature effects, may be reduced. However, from Table 3, we see that the reduction in $r_s\{v_d, \tau_d\}$ and $r_s\{v_d, F\}$ (with respect to predicted values), to first order, does not depend on the value of $r_s\{v_d, dt/dv\}$. No quantitative theoretical

TABLE 4

CORRELATION RESULTS OF THE COMBINED DATA[a]

Number (1)	Pulsar (2)	$r_s\{v_d, \tau_d\}$ (3)	$r_s\{v_d, F\}$ (4)	$r_s\{\tau_d, F\}$ (5)	$r_s\{v_d, dt/dv\}$ (6)
1.....	PSR B0823+26	$+0.57^{+0.75}_{+0.25}$	$+0.12^{+0.38}_{-0.19}$	$+0.28^{+0.55}_{-0.10}$	$-0.33^{-0.05}_{-0.62}$
2.....	PSR B0834+06	$+0.27^{+0.44}_{+0.08}$	$+0.00^{+0.16}_{-0.17}$	$+0.33^{+0.47}_{+0.17}$	$-0.49^{-0.34}_{-0.64}$
3.....	PSR B1133+16	$+0.58^{+0.77}_{+0.14}$	$+0.04^{+0.26}_{-0.23}$	$+0.07^{+0.28}_{-0.14}$	$-0.49^{-0.25}_{-0.65}$
4.....	PSR B1919+21	$-0.10^{+0.12}_{-0.31}$	$-0.12^{+0.11}_{-0.35}$	$+0.23^{+0.41}_{+0.00}$	$-0.69^{-0.56}_{-0.79}$

[a] For pulsars with multiple observing sessions.

predictions are available for the correlation between v_d and dt/dv. But our data suggest that there is some connection between the fluctuations of these two quantities.

4.3. *Stability of Correlations and Effect of Statistical Quality*

For pulsars PSR B0823+26, PSR B0834+06, PSR B1133+16, and PSR B1919+21, we have carried out correlation analysis of each distinct observing session separately, and we find that the correlation properties are not stable between successive observing sessions. PSR B0823+26(I) shows only the $\{v_d, \tau_d\}$ correlation, whereas all three combinations are correlated for PSR B0823+26(II). Data of PSR B0834+06 are even more remarkable. PSR B0834+06(I) shows correlations between all three combinations, whereas an anticorrelation between v_d and F and insignificant correlations of the other two combinations are seen for PSR B0834+06(II). For PSR B0834+06(III), the fluctuations of all three quantities are uncorrelated to each other, and PSR B0834+06(IV) shows an entirely different behavior ($\{v_d, \tau_d\}$ and $\{\tau_d, F\}$ are positive and $\{v_d, F\}$ is negative). For PSR B1133+16, qualitatively similar correlations are seen for data from sessions II and III: positive correlation between v_d and τ_d and a lack of flux correlations. However, the strength of correlation between v_d and τ_d ($r_s\{v_d, \tau_d\}$) is significantly reduced in session III compared to that in session II ($0.83 \rightarrow 0.32$), which is probably due to an underestimation of some of the v_d values in session III (see Paper I for details). For PSR B1919+21, flux correlations are absent in session I and are significant in session II. Further, $r_s\{v_d, \tau_d\}$ is considerably larger in session II

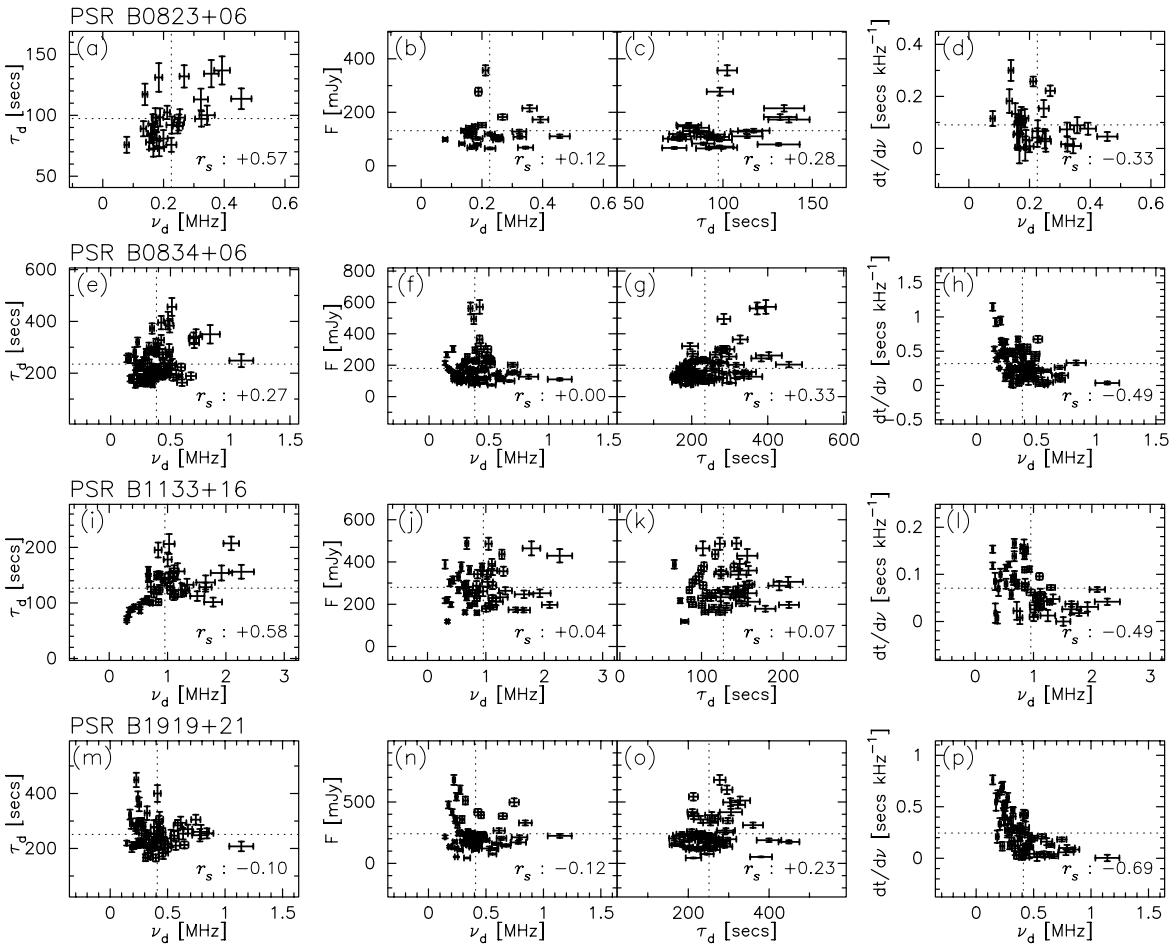

FIG. 3.—Correlation properties of four pulsars PSR B0823+26, PSR B0834+06, PSR B1133+16, and PSR B1919+21. The data from different observing sessions are combined to improve the statistical quality and reliability of the data (in terms of N_{ep} and N_{ref}). The panel description is similar to that for Fig. 1.

($0.21 \rightarrow 0.44$). All four pulsars, however, consistently show an anticorrelation between the fluctuations of v_d and dt/dv, albeit with varying magnitude.

In order to examine the effect of statistical quality of the data on the stability of correlation properties, we carried out the correlation analysis for the combined data from all the observing sessions of each pulsar. The results are given in Table 4, and the relevant scatter plots are shown in Figures 3*a*–3*p*. This procedure should have resulted in improved correlations and better agreement with the theoretical predictions, if the statistical quality of the data was the main cause for change in the correlation properties. On the contrary, it leads to reduced correlations, and sometimes even a reversal of the sense of correlation. For PSR B0823+26, the flux correlations reverse the sign on combining data from the two sessions (Figs. 3*b* and 3*c*). On combining the data from all four sessions, PSR B0834+06 shows a degradation of the $\{v_d, \tau_d\}$ correlation (Fig. 3*e*) while retaining the positive correlation between τ_d and F (seen for sessions I and IV) (Fig. 3*g*). In addition, the $\{v_d, F\}$ correlation totally vanishes ($r_s\{v_d, F\} = 0$) (Fig. 3*f*). For PSR B1133+16, flux correlations do not turn up even with the combined data (from sessions II and III) (Figs. 3*j* and 3*k*). Quite peculiar changes are seen with PSR B1919+21, where the $\{v_d, \tau_d\}$ and $\{v_d, F\}$ correlations reverse the sign (Figs. 3*m* and 3*n*), while the positive correlation between τ_d and F turns more significant (Fig. 3*o*). Thus, improvement in the statistical quality of the data, in terms of number of epochs of observation ($N_{\rm ep}$) or number of refractive cycles spanned ($N_{\rm ref}$), does not result in a better agreement with predictions and, therefore, is not likely to be the cause of the lack of stability seen with the correlation properties.

5. DISCUSSION

Although several consequences due to RISS are amply supported by our data (Papers I and II), the cross-correlation properties between the fluctuations of various scintillation observables (v_d, τ_d, dt/dv, and F), do *not fully* agree with the existing predictions. Interestingly, there are several characteristics that are common for many data sets. For example, the predicted positive correlation between decorrelation bandwidth (v_d) and scintillation timescale (τ_d) are seen with 17 of the 19 statistically reliably data sets (see Table 3 for details), whereas the general disagreement with the predictions is mainly due to poor flux correlations. However, in contrast to the predictions, the measured correlation coefficient $r_s\{v_d, \tau_d\}$ varies over a very wide range: from 0.21 [for PSRB 1919+21(I)] to 0.83 [for PSR B1133+16(II)]. Further, a fairly good number of correlations (20 of 25) are seen between the fluctuations of decorrelation bandwidth (v_d) and the drift slope (dt/dv). A broad conclusion that can be drawn from these results is that the modulations of the quantities v_d, τ_d, and dt/dv are somewhat in accordance with the theoretical expectations, while the flux variations appear to be rather more complex.

The complexity of the results seems to be beyond the scope of simple models of refractive scintillation. A satisfactory model needs to explain (1) the observed diverse nature of correlation properties, (2) poor flux correlations, and (3) much wider ranges in the strengths of correlations than the existing predictions.

Our attempts at finding a possible connection between the observed correlation properties and properties related to scattering (such as the strength of scattering [C_n^2, u], modulation indices [of v_d, τ_d, and F], and rms refractive angle [$\delta\theta_{\rm ref}$]) or pulsars (such as DM, distance, and direction [l, b]) have not been, so far, successful. For the given number of pulsars and the diversity seen with the correlation properties, individual treatments of pulsars appear rather formidable. In this section, we examine possible ways of reconciling the results from our correlation analysis and the predictions from the theory. First, we briefly address the issue of effects due to various identifiable noise sources on our correlation results (§ 5.1) and then examine the implications of the present data on intrinsic flux variations (§ 5.2). We also consider the role of persistent drifting bands on modifying the correlation properties (§ 5.3). Finally, on the basis of observational evidence(s) available, we emphasize the need for reconsidering some of the basic assumptions made by the theoretical models (§ 5.4).

5.1. *Effects due to Noise Sources*

The error bars on the sample data displayed in Figures 1*a*–1*l* and 2*a*–2*c* give some idea of the typical uncertainties due to noise sources associated with our measurement procedure. These noise sources can potentially modify the correlation properties between the various quantities and lead to a reduction in the strength of correlation. To understand this effect, we model the observed time series, $x_{\rm obs}$, as a combination of the true variable, $x_{\rm iss}$, and a noise source, x_n:

$$x_{\rm obs}(i) = x_{\rm iss}(i) + x_n(i)\ , \tag{3}$$

where x represents the quantity v_d, τ_d, or F at the ith epoch of observation. The various kinds of noise sources relevant for each quantity can be combined to obtain a net uncertainty (σ_n), given by

$$\sigma_n = \left(\sum_{j=1}^{j=k} \{\sigma_{n,j}\}^2 \right)^{0.5} . \tag{4}$$

Here $\sigma_{n,j}$ is the uncertainty caused by the jth noise source, and k is the number of independent noise sources relevant for the quantity under consideration. The sources of noise that are identifiable for our data include (1) errors due to the Gaussian model fitting to the autocorrelation functions of dynamic spectra, $\sigma_{\rm mod}$ (for v_d, τ_d, and dt/dv); (2) statistical errors due to finite number of scintles, $\sigma_{\rm est}$ (for v_d, τ_d, dt/dv, and F); (3) calibration error, $\sigma_{\rm cal}$ (for F); (4) errors due to variable ionospheric Faraday rotation, $\sigma_{\rm pol}$ (for F); (5) errors due to Earth's orbital motion, $\sigma_{v,\rm obs}$ (for τ_d); and (6) errors due to the bulk flow of the density irregularities, $\sigma_{v,\rm irr}$ (for τ_d). Typical error estimates due to these are summarized in Table 5 (see Papers I and II for the methods of estimation). We adopt a conservative value of 10% for $\sigma_{\rm cal}$. The net error due to all noise sources, σ_n, is given in columns (8), (9), and (10) of Table 5 for v_d, τ_d, and F, respectively.

We have examined the effect of these noise sources by carrying out a correlation analysis of the modified time series given by

$$x_{\rm mod}(i) = x_{\rm obs}(i) \pm f\sigma_n(i) \qquad 0 \le f \le 1 \tag{5}$$

in which $x_{\rm mod}$ is taken to be a randomly selected value ranging from $x_{\rm obs} - \sigma_n$ to $x_{\rm obs} + \sigma_n$ with uniform probability. The rank correlation coefficient is computed for all three combinations ($\{v_d^m, \tau_d^m\}$, $\{v_d^m, F^m\}$, and $\{\tau_d^m, F^m\}$, where v_d^m, τ_d^m, and F^m denote the new time series of v_d, τ_d, and F, respectively) of this modified time series. A large number

TABLE 5

EFFECTS OF NOISE SOURCES ON CORRELATION RESULTS

							σ_n			r_s^m		
NUMBER (1)	PULSAR (2)	$\sigma_{\rm mod}$ [a] (%) (3)	$\sigma_{\rm est}$ [b] (%) (4)	$\sigma_{\rm pol}$ [c] (%) (5)	$\sigma_{v,\rm obs}$ [d] (%) (6)	$\sigma_{v,\rm irr}$ [e] (%) (7)	(v_d) (%) (8)	(τ_d) (%) (9)	(F) (%) (10)	$\{v_d^m, \tau_d^m\}$ (11)	$\{v_d^m, F^m\}$ (12)	$\{\tau_d^m, F^m\}$ (13)
1	PSR B0329+54	8	5	0	3	5	9	11	11	...		−0.46
2	PSR B0628−28	9	6	2	3	6	11	13	12	0.26	−0.29	−0.41
3	PSR B0823+26(I)	14	5	18	5	4	15	16	21	0.42	...	...
4	PSR B0823+26(II)	14	4	18	10	4	15	18	21	0.22	−0.14	−0.21
5	PSR B0834+06(I)	6	9	1	14	6	11	19	13	0.31	0.29	0.28
6	PSR B0834+06(II)	6	7	1	12	5	9	16	12	−0.10	−0.18	...
7	PSR B0834+06(III)	6	6	1	5	4	8	11	12	...	...	...
8	PSR B0834+06(IV)	6	7	1	9	4	9	13	12	0.31	−0.20	0.14
9	PSR B0919+06	16	5	14	2	2	17	17	18	0.44	−0.11	−0.18
10	PSR B1133+16(I)	7	7	10	6	3	10	12	16	0.80	−0.25	...
11	PSR B1133+16(II)	7	7	10	6	3	10	12	16	0.71	...	...
12	PSR B1133+16(III)	7	6	10	4	3	9	10	15	0.20	...	...
13	PSR B1237+25	7	11	38	4	3	13	14	41	0.35	0.82	0.27
14	PSR B1508+55	17	4	1	0	2	17	18	11	0.28	−0.44	−0.65
15	PSR B1540−06	11	5	17	24	13	12	30	20	...	0.44	...
16	PSR B1604−00	5	10	5	24	16	11	31	15	0.09	...	−0.16
17	PSR B1747−46	13	4	10	3	5	14	15	15	0.21	...	...
18	PSR B1919+21(I)	5	8	18	2	8	9	13	22	0.13	...	...
19	PSR B1919+21(II)	5	9	18	5	5	10	12	22	0.13	0.18	−0.06
20	PSR B1929+10	6	16	49	6	7	17	19	53	...	0.53	−0.08
21	PSR B2016+28	6	12	2	14	18	13	26	16	0.24	−0.12	0.11
22	PSR B2020+28	8	5	1	2	5	9	11	11	0.23	−0.22	−0.28
23	PSR B2045−16	12	6	4	5	2	13	14	12	...	...	...
24	PSR B2310+42	13	5	4	4	11	14	18	12	...	−0.62	...
25	PSR B2327−20	4	8	3	22	13	9	27	13	...	0.07	0.27

[a] Typical errors on the quantities v_d and τ_d.
[b] Typical errors on the quantities v_d, τ_d, and F.
[c] The ionospheric contribution to the rotation measure is assumed to be ~ 1 rad m^{-2}.
[d] For the net change ($\Delta V_{\rm obs_\perp}$) in the transverse component of Earth's orbital motion during the time span of observation.
[e] On assuming a motion of ~ 10 km s^{-1} (Bondi et al. 1994) for the density irregularities.

(~ 1000) of such time series have been analyzed, and the average value of all the correlation coefficients is treated as the modified correlation coefficient, r_s^m. The results obtained in this manner are tabulated in columns (11), (12), and (13) of Table 5. Comparison with the corresponding numbers in Table 3 shows that the reduction in degrees of correlations due to above-mentioned noise sources varies from a few percent to as large as 50%. This indicates that the underlying noise sources can be responsible for the reduced degrees of correlations (at least for some cases), but they cannot explain the lack of significant correlations (i.e., $|r_s| \lesssim 0.1$) or a reversal of the sense of correlation. This is consistent with the fact that the modulations due to these noise sources are much smaller than the measured depths of modulations of the quantities. Our analysis also shows the magnitudes of noise required for a substantial reduction in the strength of correlation, or a complete elimination of the existing correlation, are such that $\sigma_n \sim 50\%$; this is illustrated in Figure 4 using the example of PSR B0628−28 data.

We note that the more basic question of the noise required to reduce the theoretically expected correlations to the observed values cannot be precisely answered by this technique. Nevertheless, our method gives ample indication that poor correlations seen in the data cannot be accounted for by the aforementioned noise sources alone. If the degrees of correlations have been reduced to their present values owing to some yet unrecognized noise sources, then they need to be such that the fractional uncertainties caused by them are much larger than their modulation indices. The presence of such noise sources seems to be quite unlikely.

5.2. *Flux Variations*

Pulsar flux variations can be broadly grouped under three categories: (1) intrinsic variations, (2) those due to DISS, and (3) those due to RISS. Intrinsic flux variations are mostly expected to take place on short timescales, with most pulsars showing random fluctuations from pulse to pulse. Almost all our data are taken over durations long enough essentially to quench such intrinsic fluctuations. Most of our data were obtained during the hours when the ionosphere was not active; therefore, a probable bias in the estimate of flux density due to ionospheric scintillations is not important. Further, even if ionospheric scintillations were present with large modulations (typically 50%) and over long timescales (~ 10 s), there will be ~ 700 independent cycles of fluctuations during our typical observing scans (~ 2 hr), thereby reducing the bias to the level of $\sim 2\%$. The effect due to residual DISS fluctuations at any epoch is already included as a noise term, as described in § 5.1. Poor flux correlations ($r_s\{v_d, F\}$ and $r_s\{\tau_d, F\}$), as seen in our data, can result from two possibilities: (1) RISS fluctuations of flux occurring on timescales different from those of v_d and τ_d or (2) flux variations on timescales similar to

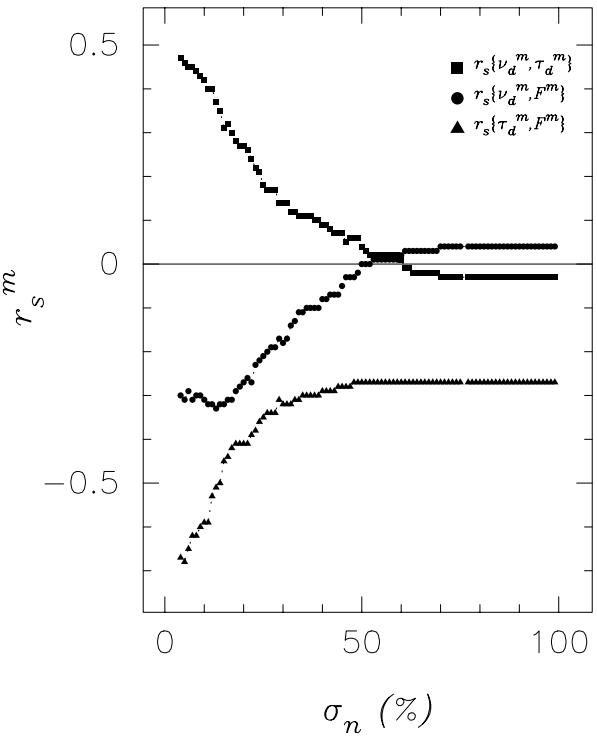

FIG. 4.—Effect of noise on the correlation properties, illustrated using the data of PSR B0628−28. Modified correlation coefficients (r_s^m) are plotted against the magnitude of noise introduced (σ_n) (in quantities v_d, τ_d, and F) for the combinations $\{v_d^m, \tau_d^m\}$, $\{v_d^m, F^m\}$, and $\{\tau_d^m, F^m\}$. The symbols used are explained at the top right-hand corner.

refractive timescales but caused by a hitherto unidentified intrinsic source.

Regarding the first possibility, we note that though the theoretical models assume that v_d, τ_d, and F vary on similar timescales, there is no conclusive observational verification of the same. Our data are not sampled regularly enough to obtain meaningful values for the fluctuation timescales of these quantities using a correlation or structure function analysis. In this context, it is interesting to note that most estimates of measured timescales for refractive flux modulations (see, e.g., Gupta et al. 1993; Spangler et al. 1993) are reported to be substantially smaller than the values predicted by theory.

Turning to the second possibility, we note that significant reductions in the flux correlations can result if, in addition to RISS modulations, there are large-amplitude intrinsic flux variations occurring over timescales comparable to refractive timescales. Using the method described in § 5.1, we have examined the effect on correlation properties of flux density by treating the possible intrinsic flux variations in the form of a "noise source." The analysis shows that substantial amounts of intrinsic flux variations will be required to produce the poor flux correlations seen in the data. The characteristics of such noise sources are found to be such that the fractional rms fluctuations due to them are quite comparable to the observed flux modulation indices (m_r). Under such conditions, the RISS-induced flux variations will have to be unusually low ($\sim$10%–15%). A simple Kolmogorov form of density spectrum implied by such low values of flux modulation indices will be, however, in contradiction with the modulation characteristics of v_d and τ_d (denoted as m_b and m_t, respectively), which suggest a spectrum steeper than $\alpha = 11/3$ (Paper II). No theory predicts a situation of large-amplitude modulations of v_d and τ_d ($m_b \sim$ 0.3–0.55 and $m_t \sim$ 0.1–0.3) and small-amplitude flux modulations ($m_r \sim$ 0.1–0.15). Thus, it is unlikely that long-term intrinsic fluctuations (if they exist) are responsible for the reduced flux correlations seen in our data.

5.3. *Effect of Persistent Slopes of Patterns*

In our earlier papers (Papers I and II), we have discussed the anomalous scintillation behavior of "persistent drift slopes" seen with PSR B0834+06 and PSR B1919+21, where the drift slope of intensity patterns in the dynamic spectra shows few or no sign reversals during the entire observing session. We also described a classification scheme, based on the statistical characteristics of drift rate measurements, to distinguish between the cases of "nonreversals" and "frequent reversals" of drift slopes. The data were accordingly categorized into class II and class I respectively, and those for which a clear distinction was not possible were categorized as "NC" (see Table 2, col. [6]). The data from the first three observing sessions of PSR B0834+06 and the two sessions of PSR B1919+21 clearly come under class II; there are six entries in "NC" and 14 in class I. Interestingly, we find none of the pulsars which shows reasonable agreement with the predictions belong to the special category, class II.

Since the traditional decorrelation bandwidth (v_d) is affected by the presence of sloping patterns in dynamic spectra, the modulation characteristics of v_d can get significantly altered due to persistent drift slopes. Consequently, this may lead to significant changes in the correlation properties of v_d with the other quantities. In Paper II, we defined a new quantity, "drift-corrected decorrelation bandwidth" (v_{d_c}), which can be treated, to first order, as v_d in the absence of refractive bending (i.e., $\theta_{\rm ref} = 0$). Therefore, in the event of drifting bands playing a substantial role in the modulations of v_d, it is reasonable to expect the correlations of v_{d_c} to differ significantly from that of v_d.

On carrying out a correlation analysis between the variations of v_{d_c} and τ_d for PSR B0834+06, for which the property of persistent drift slopes is extensively seen, we find the results to be considerably different from that of the combination v_d and τ_d (see Table 6). Scatter plots illustrating this are shown in Figures 5*a*–5*h*, where plots of v_d versus τ_d and v_{d_c} versus τ_d are displayed for four sessions of PSR B0834+06 to highlight the change of trend on using v_{d_c}. Interestingly, the new correlations of PSR B0834+06(II) and PSR B0834+06(III) are in qualitative agreement with the prediction for bandwidth-time correlation (Figs. 5*d* and 5*f*), although quantitative discrepancy prevails. Also, for PSR B0834+06(I), the method yields a considerable enhancement of the bandwidth-time correlation—$r_s\{v_d, \tau_d\} = 0.44 \rightarrow r_s\{v_{d_c}, \tau_d\} = 0.59$, which agrees with the theoretical value within the 90% confidence limits (Figs. 5*a* and 5*b*). No such improvement is seen for PSR B0834+06(IV) (i.e., $r_s\{v_d, \tau_d\} \approx r_s\{v_{d_c}, \tau_d\}$) (Figs. 5*g* and 5*h*) which shows drift reversals like many other pulsars. Thus it appears that the method gives some meaningful results for data with persistent sloping patterns.

On applying this analysis to the data of another class II pulsar, PSR B1919+21, we find that the improvements in the correlations are only marginal. But we also note that these data are comparatively weaker examples of persistent drifts and are characterized by occasional sign reversals of

TABLE 6

CORRELATION PROPERTIES OF THE DRIFT-CORRECTED DECORRELATION BANDWIDTH

Data	Decorrelation Bandwidth and Scintillation Timescale $r_s\{\nu_d, \tau_d\}$	Corrected Decorrelation Bandwidth and Scintillation Timescale $r_s\{\nu_{d_c}, \tau_d\}$
PSR B0834+06(I).....	$+0.44^{+0.66}_{+0.09}$	$+0.59^{+0.75}_{+0.28}$
PSR B0834+06(II).....	$-0.14^{+0.22}_{-0.58}$	$+0.35^{+0.62}_{-0.08}$
PSR B0834+06(III).....	$+0.07^{+0.44}_{-0.44}$	$+0.29^{+0.55}_{-0.14}$
PSR B0834+06(IV).....	$+0.42^{+0.65}_{+0.01}$	$+0.43^{+0.65}_{+0.06}$
PSR B2310+42	$-0.04^{+0.56}_{-0.68}$	$+0.59^{+0.79}_{-0.25}$

drifts (Paper I). For completeness, we carried out a similar analysis for data classified into other two categories, the results from which are summarized in Figures 6*a*–6*c*. Here the correlation coefficients between the fluctuations of ν_{d_c} and τ_d ($r_s\{\nu_{d_c}, \tau_d\}$) are plotted against those between the fluctuations of ν_d and τ_d ($r_s\{\nu_d, \tau_d\}$). The changes in the correlation properties are found to be only marginal for class I data, except for PSR 2327−20, which may be a spurious effect resulting from the systematic trend present in the time series of τ_d for this pulsar (Fig. 4*x* of Paper I). But among the data classified as "NC," PSR B2310+42 was found to be an exception in which the method leads to a significant enhancement in bandwidth-time correlation ($r_s\{\nu_d, \tau_d\} = 0.04$, whereas $r_s\{\nu_{d_c}, \tau_d\} = 0.59$), bringing it within reasonable agreement with the predictions. Interestingly, from the time series of drift rate measurements (Fig. 4*w* of Paper I), it appears that this pulsar is similar to PSR B0834+06 and PSR B1919+21, though a clear distinction was not possible owing to the poor statistical quality of its data.

Figures 6*b* and 6*c* summarize the other correlations of ν_{d_c}, i.e., $\{\nu_{d_c}, F\}$ and $\{\nu_{d_c}, dt/dv\}$. In Figure 6*b*, $r_s\{\nu_{d_c}, F\}$ is plotted against $r_s\{\nu_d, F\}$. Barring a few exceptions (indicated with the corresponding pulsar name alongside), we find the new correlation coefficients to be only marginally different from those between the traditional decorrelation bandwidth and flux density. By and large, this seems to be in accordance with the simple expectations based on the existing RISS models, where the flux correlations are expected to arise from curvature effects and, therefore, should not be affected by the drift slopes. However, we note that PSR B0834+06 (I, II and III) and PSR B2310+42, which show an improved correlation for $\{\nu_{d_c}, \tau_d\}$, do not show a similar improvement for $\{\nu_{d_c}, F\}$. A plot of $r_s\{\nu_{d_c}, dt/dv\}$ against $r_s\{\nu_d, dt/dv\}$ is shown in Figure 6*c*. Values of the new correlation coefficients are consistently biased above the line of unity slope, which means a significant reduction in the coefficient or a reversal of the sense. Such a behavior is well in accordance with our presumption that the observed anticorrelation between ν_d and dt/dv results from the reduction in ν_d due to refractive gradients, and, hence, poorer correlations should result between the drift-corrected ν_d and dt/dv.

Although the present analysis does not firmly establish the exact role of persistent drifts in modifying the correlation properties, it provides some evidence for refractive modulations getting considerably modified in the presence of persistent drifts. Modulation characteristics under such scenarios are not worked out by the available theoretical models for RISS. In any case, persistent pattern drifts seem

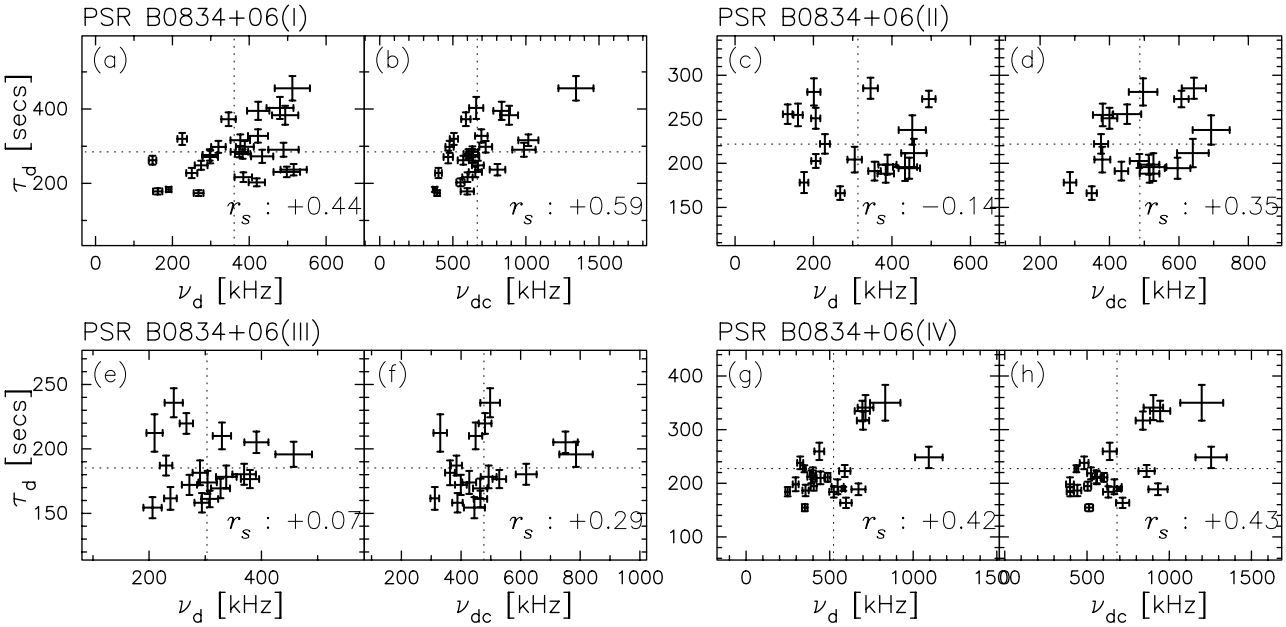

FIG. 5.—Effect of persistent drifting bands on the bandwidth-time correlation of PSR B0834+06. The panel description is similar to that in Fig. 1. There are two panels each for the data from a given session; the first one is the scatter plot of traditional ν_d against τ_d, while the second one is for the drift-corrected ν_d (ν_{d_c}) against τ_d.

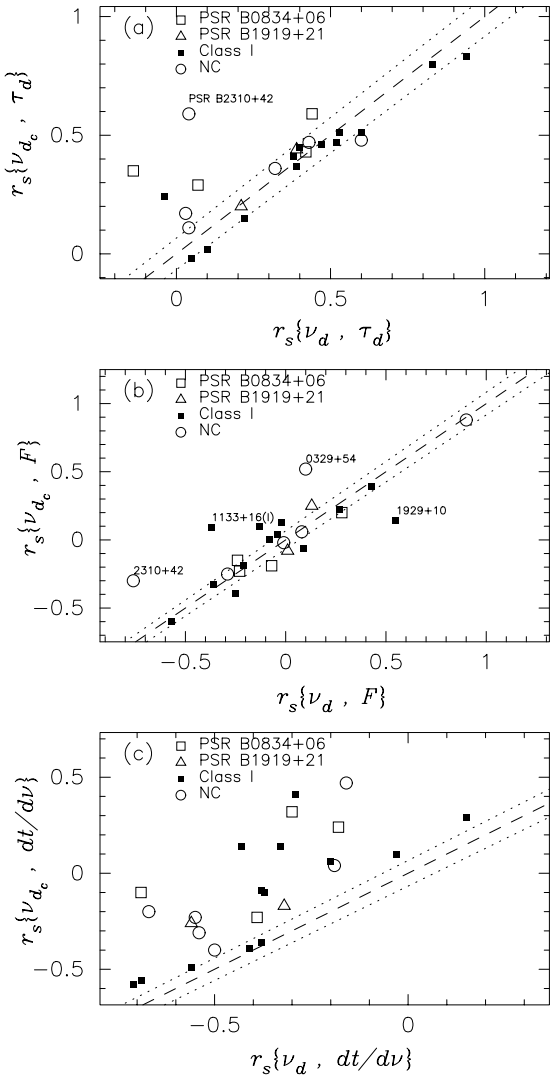

FIG. 6.—Results of the correlation analysis of drift-corrected decorrelation bandwidth ν_{d_c}. (*a*) Correlation coefficients between ν_{d_c} and τ_d are plotted against those between ν_d and τ_d. (*b*) Correlation coefficients between ν_{d_c} and F are plotted against those between ν_d and F. (*c*) Correlation coefficients between ν_{d_c} and dt/dv are plotted against those between ν_d and dt/dv. The dashed line is of unity slope, and dotted lines define a band of 10% discrepancy. The symbols used are explained inside the figure itself.

to be another plausible reason which can reduce the true correlations due to "normal RISS," thereby giving rise to inconsistencies with the predictions.

5.4. *Limitations and Possible Improvements of Theories*

The overall inconsistency of the present observations with theoretical predictions also raises the question of validity of some of the basic assumptions usually made by the theoretical models. Here we address some of them that may be relevant for suitable refinements of the existing models.

5.4.1. *Effect of Extended and Inhomogeneous Media*

Most of the available theoretical calculations, including cross-correlation properties between scintillation observables, have been confined to the simplest scenario of thin screen scattering models. Romani et al. (1986) show that the thin screen theory underestimates the refractive flux fluctuations by a factor $\sim$1.4–2.3 (depending on the power-law index of the density irregularity spectrum) in comparison to a continuously distributed scattering medium. Such detailed treatments are not available for the rest of the observables. It is worth investigating how the correlation properties will be altered on considering more realistic scattering geometries (such as multiple screens or a continuous medium). Our data show that the measured flux density modulation indices are in better agreement with the theoretical predictions of an extended scattering medium than those of a thin screen (Paper II). Therefore, it is possible that the agreement between the observed correlation properties and the predictions can also improve upon taking into consideration the effects due to extended medium. Further, the extended geometry generally considered by the models is that of a homogeneous distribution of scattering material in the line of sight. Not much understanding exists on strong scattering effects due to a heterogeneous distribution of scattering material.

The ISM is known to be of clumpy nature in general, and there are regions (such as supernova shocks, H II regions, etc.) in which the strength of scattering is much larger than that in a typical region of the ISM. Cordes et al. (1988b, 1991) suggested the need for a clumped, intense component with a volume filling factor $\approx 10^{-4} R_{\rm pc}$ (where $R_{\rm pc}$ is the size of clump) for the Galactic distribution of turbulence. The strength of turbulence is believed to be 3–4 orders of magnitude larger in this clump component. However, since the present study has been restricted largely to close-by ($\lesssim$1 kpc) pulsars, scattering effects due to this component or those due to the Galactic spiral arms may not be important for most of our pulsars.

Interestingly, our data have also shown evidence for a highly inhomogeneous distribution of scattering material in the LISM (Bhat et al. 1997, 1998), in which a scattering structure of a bubble with a shell boundary is suggested for the solar neighborhood. On examining the contributions to the scattering from different components, viz., the cavity (i.e., interior of the bubble), the shell, and the outer ISM, we find the lines of sight to the pulsars can be broadly categorized into four groups: (1) predominant scattering ($\gtrsim$75%) due to the outer ISM (class A); (2) substantial contributions from both the shell as well as the outer ISM (class B); (3) scattering due to the shell and the outer ISM, but predominantly ($\gtrsim$70%) due to the former (class C); and (4) scattering due to the entire line of sight, in which the cavity also contributes significantly in addition to the shell and the outer ISM (class D). Classification of pulsars according to this scheme (Table 2, col. [7]) shows that pulsars, for which the observed correlations are in reasonable agreement with the predictions, do not come under any specific class. However, we note that, in our data, the agreement with the predictions is generally seen for pulsars with comparatively larger DMs (20–35 pc cm^{-3}). While we are unable to identify any simple connection between the diversity of the correlation results and the structure of the LISM, it is plausible that the observed correlations are manifestations of some hitherto unrecognized ISS effects, presumably relevant in the case of heterogeneous media.

Over the past several years, observations have revealed various kinds of unusual scattering effects (such as multiple imaging events, ESEs, and persistent drifts) that are attributed to the presence of large-scale dense refracting structures in the ISM (see, e.g., Cordes & Wolszczan 1986;

Rickett, Lyne, & Gupta 1997; Fiedler et al. 1987, 1994; Gupta et al. 1994; Paper II). While details such as their possible associations with other Galactic structures and the distribution in the Galaxy still remain to be understood, the accumulated data give some indication of their important role in ISS of pulsars and radio sources. It is worth mentioning that two of these, ESEs and persistent drifts, occur over timescales comparable to or longer than refractive timescales and hence can potentially modify the time series of some of the scintillation observables and may even alter the cross-correlations between their fluctuations. There is some evidence in support of this view from the present study and from Lestrade, Rickett, & Cognard (1998). While our analysis shows persistent drift slopes modifying the correlations between v_d, τ_d, and dt/dv (§ 5.3), Lestrade et al. (1998) discuss the effect of ESEs on the correlation between flux density and the pulse arrival time. A recent paper by Clegg, Fey, & Lazio (1998) (also see Romani, Blandford, & Cordes 1987; Fiedler et al. 1994) analyzes the characteristics of flux variations due to discrete plasma lensing structures. There are no theoretical treatments at present that address the perturbations on DISS observables due to such structures. But there is some observational evidence to suggest that the role of discrete structures may be important in the cross-correlation properties of some of the observables.

5.4.2. *Refractive Effects and the Electron Density Spectrum*

As mentioned in § 2, the cross-correlation properties of the scintillation observables have been worked out for simple power-law forms of density fluctuation spectra. Several attempts have been made in the recent past to determine the exact form of the spectrum, but a conclusive picture is yet to emerge. There are conflicting results from various kinds of measurements (see Paper II; Armstrong, Rickett, & Spangler 1995; Rickett 1990; Narayan 1988). There are observations indicating that a simple power-law description is inadequate and that the spectrum needs to be more refractive in nature than a simple Kolmogorov form. Furthermore, there is substantial evidence (mainly from phenomena such as multiple imaging, ESEs, and persistent drifts) which suggests the existence of localized dense refracting structures in the ISM, thereby favoring *non–power-law* forms of spectrum, at least for some lines of sight. Some viable options as indicated by our observations and several others from the literature are (1) a *composite* spectrum that steepens at low wavenumbers ($\sim 10^{-14}$ to 10^{-11} m^{-1}), (2) a power-law form of spectrum (with $\alpha \approx 11/3$) in combination with a separate large-scale (say, $\sim$10–100 AU) component, and (3) a power-law spectrum superposed with dense discrete structures. According to Romani et al. (1986), if the density spectrum has a simple power-law form (i.e., with unimportant cutoffs), then correlations between the fluctuations of v_d, τ_d, and F are qualitatively similar for different values of spectral slope (α). But it is quite possible that, like several other refractive effects, correlation properties also turn highly sensitive to the spectral characteristics when the spectrum has a more complex form. Theoretical developments in this direction remain to be made.

5.4.3. *Nonstationarity of the Medium*

Another observational result of interest is the evidence for an apparent lack of stability of the observed correlation properties. We have four pulsars with multiple, well-separated observing sessions spanning $\sim$1–3 yr, and their correlation properties are found to be changing significantly from session to session. The property is best illustrated by the data of PSR B0834+06, observations of which span a period of $\sim$1000 days (four sessions), and substantial variations are seen between any two successive sessions. In § 4.3, we showed that this effect is not due to the statistical quality of the data—in terms of number of epochs of observation ($N_{\rm ep}$) and number of refractive cycles spanned ($N_{\rm ref}$). Such an effect is unexpected if the ISM was well behaved and the underlying density fluctuations were describable by a simple power-law spectrum. We also note that the changes in correlation properties are sometimes accompanied by substantial changes in the diffractive and/or refractive scintillation properties (Papers I and II). While the observed variations of v_d and τ_d are explainable, in some cases, in terms of variations in the scattering strength (C_n^2) or in the pattern velocity ($V_{\rm iss}$), it is not very obvious what kind of effects can lead to the variations seen in the correlation properties. Long-term variations of this kind are difficult to understand in terms of simple models and point to some hitherto unrecognized form of ISS or a more complex nature of the scattering medium. If such variations are to be attributed to the medium, then the present observations do not support the assumption of a stationary medium.

6. CONCLUSIONS

We have analyzed data from our long-term pulsar observations to test the quantitative predictions given by the theoretical models of refractive scintillation. The data consist of dynamic scintillation spectra for 18 pulsars, which were regularly monitored at 10–90 epochs over time spans $\sim$100–1000 days. They allow simultaneous measurements of the observables decorrelation bandwidth (v_d), scintillation timescale (τ_d), drift rate of the intensity patterns (dt/dv), and flux density (F). The observed fluctuations of these quantities are examined for their cross-correlation properties and are compared with the existing predictions. For five pulsars, there is reasonable agreement with the predictions, where a positive correlation between v_d and τ_d and anticorrelations between v_d and F, and τ_d and F, are seen. The measured degrees of correlations are, however, generally lower than the predicted values. While a number of data sets (roughly 60%) show "partial agreement" (i.e., one to two combinations in qualitative agreement with the predictions, while an absence or an opposite correlation is the case with the remaining ones), there are also examples [PSR B0834+06(III) and PSR B2045−16] for which the variations of all three quantities are uncorrelated to each other. A complexity of this kind is not easy to comprehend in terms of simple models.

Despite the inconsistency of the correlation results with the predictions, there are some general trends. A large number of pulsars show positive correlations between the fluctuations of decorrelation bandwidth and scintillation timescale, while the disagreement is mainly due to the poor flux correlations. Another interesting result is the anticorrelation seen between the fluctuations of decorrelation bandwidth and drift slope for many pulsars. Although the relevant quantitative predictions are not available at present, the observed behavior is in accordance with the expectations based on the simple models of RISS.

The statistical quality of the data does not seem to be the cause of the inconsistency with the theoretical predictions, as an improved statistics (for pulsars with multiple observ-

ing sessions) does not result in a better agreement with the predictions. Our analysis shows, for part of the data, the underlying noise sources might be responsible for reduced correlation coefficients. Nevertheless, they cannot explain the absence of significant correlations seen with a substantial (roughly one-third) part of the data. Our analysis suggests it is unlikely that the observed poor flux correlations arise from hitherto unrecognized large-amplitude intrinsic flux variations occurring on timescales similar to that of refractive fluctuations. Further, we find the anomalous scintillation behavior such as persistent drift slopes to be the cause of lack of correlations for part of the data (sessions II and III of PSR B0834+06 and PSR B2310+42), where the predicted positive correlation between v_d and τ_d turns up on using the drift-corrected v_d.

The qualitative agreement between the observed and predicted correlations for a number of pulsars indicates that our basic understanding of refractive scintillation is correct. However, reduced correlation coefficients and the absence of one or more of the predicted correlations suggests that in actual practice, conditions are more complex than assumed by the theoretical models. Some of the basic assumptions such as the thin-screen approximation and a simple power-law description of irregularity spectrum need to be reexamined. The theory also needs to be enhanced to take into account nonuniform distribution of scattering along the line of sight. A more comprehensive theory incorporating these and additional features needs to be evolved to explain the observed complexities. We hope the present observations will stimulate further theoretical work toward a better understanding of various refractive scattering phenomena due to the ISM.

The authors wish to thank J. Chengalur and R. T. Gangadhara for reading the manuscript and giving useful comments. We thank our referee for several fruitful comments and suggestions toward improving the presentation of our results in this paper.

REFERENCES

Armstrong, J. W., Rickett, B. J., & Spangler, S. R. 1995, ApJ, 443, 209
Bhat, N. D. R., Gupta, Y., & Rao, A. P. 1997, in Lecture Notes in Physics, 506, IAU Colloq. 166, The Local Bubble and Beyond, ed. D. Breitschwerdt, M. J. Freyberg, & J. Trümper (Berlin: Springer), 211
———. 1999a, ApJ, in press (Paper I)
———. 1999b, ApJ, 514, 249 (Paper II)
Bhat, N. D. R., Rao, A. P., & Gupta, Y. 1998, ApJ, 500, 262
Blandford, R. D., & Narayan, R. 1985, MNRAS, 213, 591
Bondi, M., Padrielli, L., Gregorini, L., Mantovani, F., Shapirovskaya, N. & Spangler, S. R. 1994, A&A, 287, 390
Clegg, A. W., Fey, A. L., & Lazio, T. J. 1998, ApJ, 496, 253
Cordes, J. M., Pidwerbetsky, A., & Lovelace, R. V. E. 1986, ApJ, 310, 737
Cordes, J. M., Rickett, B. J., & Backer, D. C., eds. 1988a, in AIP Conf. Proc. 174, Radiowave Scattering in the Interstellar Medium, ed. J. M. Cordes, B. J. Rickett, & D. C. Backer (New York: AIP)
Cordes, J. M., Spangler, S. R., Weisberg, J. M., & Clifton, T. R. 1988b, in AIP Conf. Proc. 174, Radiowave Scattering in the Interstellar Medium, ed. J. M. Cordes, B. J. Rickett, & D. C. Backer (New York: AIP), 180
Cordes, J. M., Weisberg, J. M., Frail, D. A., Spangler, S. R., & Ryan, M. 1991, Nature, 354, 121
Cordes, J. M., & Wolszczan, A. 1986, ApJ, 307, L27
Diaconis, P., & Efron, B. 1983, Sci. Am., 24(5), 116
Efron, B. 1979, Ann. Stat., 7, 1
Fiedler, R. L., Dennison, B., Johnston, K. J., & Hewish, A. 1987, Nature, 326, 675
Fiedler, R. L., Dennison, B., Johnston, K. J., Waltman, E. B., & Simon, R. S. 1994, ApJ, 430, 581
Gould, D. M. 1994, Ph.D. thesis, Univ. of Manchester
Gupta, Y., Rickett, B. J., & Coles, W. A. 1993, ApJ, 403, 183
Gupta, Y., Rickett, B. J., & Lyne, A. G. 1994, MNRAS, 269, 1035
Hewish, A. 1992, Philos. Trans. R. Soc. London, A341, 167
Kaspi, V. M., & Stinebring, D. R. 1992, ApJ, 392, 530
Lestrade, J., Cognard, I., & Biraud, F. 1995, in ASP Conf. Proc. 72, Millisecond Pulsars: A Decade of Surprise, ed. A. Fruchter, M. Tavani, & D. Backer (San Francisco: ASP), 375
Lestrade, J., Rickett, B. J., & Cognard, I. 1998, A&A, 334, 1068
Narayan, R. 1988, in AIP Conf. Proc. 174, Radiowave Scattering in the Interstellar Medium, ed. J. M. Cordes, B. J. Rickett, & D. C. Backer (New York: AIP), 17
———. 1992, Philos. Trans. R. Soc. London, A341, 151
Press, W. H., Flannery, B. P., Teukolsky, S. A., & Vetterling, W. T. 1992, Numerical Recipes—The Art of Scientific Computing (Cambridge: Cambridge Univ. Press)
Rickett, B. J. 1990, ARA&A, 28, 561
Rickett, B. J., Coles, W. A., & Bourgois, G. 1984, A&A, 134, 390
Rickett, B. J., Lyne, A. G., & Gupta, Y. 1997, MNRAS, 287, 739
Romani, R. W., Blandford, R. D., & Cordes, J. M. 1987, Nature, 328, 324
Romani, R. W., Narayan, R., & Blandford, R. D. 1986, MNRAS, 220, 19
Sieber, W. 1982, A&A, 113, 311
Spangler, S. R., et al. 1993, A&A, 267, 213
Stinebring, D. R., Faison, M. D., & McKinnon, M. M. 1996, ApJ, 460, 460
Wolszczan, A., & Cordes, J. M. 1987, ApJ, 320, L35